

Molecular modeling of RecX reveals its mode of interaction with RecA

Subhra Mishra,^a Pooja Anjali Mazumdar,^a Joykrishna Dey,^b and Amit Kumar Das^{a,*}

^a Department of Biotechnology, Indian Institute of Technology, Kharagpur 721302, India

^b Department of Chemistry, Indian Institute of Technology, Kharagpur 721302, India

Received 15 October 2003

Abstract

The protein RecA is involved in homologous recombination, DNA repair and also catalyzes DNA strand exchange. RecX gene is downstream of recA and the gene product RecX is supposed to be important for RecA regulation. Recombinant RecX is purified to homogeneity, and circular dichroism (CD) and FTIR spectroscopy show the protein to exist mostly in helical conformation. The fluorescence emission maxima of the native and the denatured protein and the steady-state fluorescence quenching studies with acrylamide indicate the presence of tryptophan residues partially exposed to the bulk solvent. Denaturation studies with urea and guanidine hydrochloride by use of spectroscopic methods, fluorescence, and CD also confirm the instability of the protein and unfolding occurs following a two-state model. Mass spectrometry and gel permeation chromatography suggest the monomeric form of the protein. Molecular modeling of RecX represents the molecule as extended and helical bundle in conformity with the spectroscopic results. To understand the mechanism of RecX in the regulation of RecA the structural model of RecA–RecX has been discussed. In this proposed model, entry of RecX into hexameric RecA filament prevents binding of ssDNA and also inhibits ATPase activity.

© 2003 Elsevier Inc. All rights reserved.

Keywords: RecX; Purification; CD; Fluorescence; FTIR; Modeling

DNA damage inside the cell is a well-known fact and in order to avoid genetic changes, cells have evolved mechanisms to repair this damage. DNA repair and recombination is intimately linked to transcription and cell cycle control. Recombination processes include homologous recombination site-specific recombination, and transposition. Among these three, RecA protein is involved in homologous recombination and catalyzes DNA strand exchange [1–4]. The RecA protein of *Escherichia coli* takes part in DNA metabolism as well as in several biological processes. The protein has evolved as the central component of a recombinational DNA repair system with the generation of genetic diversity being a useful byproduct. Its three-dimensional structure has shown it to be involved in DNA strand exchange [5]. It also binds to ssDNA and activates the protein cleaving activity of LexA repressor. The SOS regulon including *recA*, activated by SOS system, inhibits cell division in order to increase the

time the cell has, to repair any damage, before DNA replication.

Recently, a gene called *recX*, downstream of *recA* gene, has been identified and it has been found to be conserved in bacteria [6]. The same genomic organization of *recX* gene as that seen in *E. coli* (*recA–recX–alaS*) has been identified in *Mycobacterium leprae*, *Mycobacterium tuberculosis*, *Vibrio cholerae*, *Thiobacillus ferrooxidans*, *Pseudomonas fluorescens*, *Pseudomonas aeruginosa* as well as other gram negative and gram positive bacteria [7–10]. Indeed, all genes which have so far been reported to display the same genomic organization, belong to the operonic structure, i.e., ribosomal RNA operons, the *cys* DNA operon involved in sulfate assimilation, and the *atpEFHAGDC* operon encoding ATP synthase. The *recX* gene overlaps with *recA* [9]. It is also reported to cotranscribe with *recA* in *Mycobacterium* species, *V. cholerae*, and *T. ferrooxidans* and is coupled to *recA* expression [9]. Overexpression of RecA is toxic in the absence of RecX. This suggests a regulatory role of RecX towards RecA [11]. Furthermore, it has been shown that the *recA* gene from some other

* Corresponding author. Fax: +91-3222-255303.

E-mail address: amitk@hijli.iitkgp.ernet.in (A.K. Das).

bacteria can only be cloned in a *recA* mutant of *E. coli* if *recX* is present in the insert. It is impossible to generate *recA*-deficient mutants due to its polar effect on *recX* gene. More recently, it has been proved that RecX of *Mycobacterium* species inhibits ATP hydrolysis by RecA [12] and RecX of *E. coli* inhibits both ATP hydrolysis and DNA binding activity of RecA [13]. However, RecX of *Neisseria gonorrhoeae* enhances RecA activity [14]. So, the RecX protein is an important candidate for controlling RecA function. This indicates the involvement of RecX in RecA function. The 3D structure of RecX will help in the understanding of the regulation of RecA.

In this work, the model three-dimensional structure of RecX has been proposed and supported by different spectroscopic results. The mechanism of action of RecX in the regulation of RecA has also been explained. This paper describes the purification, spectroscopic characterization, molecular modeling of RecX and also proposes a model for the interaction of RecX with RecA.

Methods

Cloning. The *recX* gene (501 bp) was amplified from *E. coli* K-12 genomic DNA using two 33 mer oligonucleotides, 5'-CCC AAG CTT TCA GTC GGC AAA ATT TCG CCA AAT-3' and 5'-CGC GGA TCC ATG ACA GAA TCA ACA TCC CGT CGC-3'. The resulting PCR products were cloned into pUC18 vectors and then into modified pET28a (modified, thrombin cleavage site has been removed) at the cloning site suitable for *Bam*HI and *Hind*III of the gene. The pET expression plasmid was transformed into B834 cells and protein was expressed by induction with IPTG.

Overexpression and purification of RecX. Overexpression and induction were studied under varying conditions of temperature (15, 20, and 37 °C) and IPTG concentration (0.15, 0.25, and 0.50 mM). LB medium containing 0.03 µg/ml kanamycin was inoculated with the stationary overnight culture. Cell pellets from 2 L were resuspended in 70 ml of lysis buffer (10 mM Tris, 10 mM imidazole, 300 mM NaCl, pH 8.0, 0.5 mg/ml lysozyme, 1 µg/ml of each of leupeptin, pepstatin, and aprotinin), lysed by sonication, and centrifuged at 15,000 rpm for 45 min at 4 °C. The supernatant was loaded onto Ni-NTA affinity column. The bound protein was then eluted using 300 mM imidazole in buffer containing 300 mM NaCl at pH 5.5. The eluent was loaded onto Sephadex G75 column (70 ml) equilibrated with the buffer containing 20 mM MES (pH 5.5) and 100 mM NaCl at a flow rate of 1 ml/min. The peak protein fractions were loaded onto an HR (5/5) Mono S cation exchanger column previously equilibrated with the same buffer. Application of a linear gradient of 40 ml from 100 mM to 1 M NaCl eluted the bound protein. Fractions were collected and analyzed on a 15% SDS-polyacrylamide gel. The amount of the total protein from each step of the purification was evaluated by the Bradford assay [15].

Determination of extinction coefficient. The extinction coefficient (ϵ) of the protein at 280 nm was calculated from the value of the extinction coefficient at 205 nm [16]. Protein concentration was calculated and used for measurement of ϵ (280 nm).

Circular dichroism study. CD spectra of the RecX protein were recorded on a Jasco J-600 CD spectropolarimeter using 0.1 cm path length quartz cell at 20 °C. Far-UV spectra were collected at a protein concentration of 5 µM in 20 mM MES (pH 5.5) and 700 mM NaCl. Data points were recorded with a step resolution of 0.2 nm, time constant of 2 s, sensitivity 10 mdeg, scan speed 50 nm/min, and a spectral bandwidth of 2.0 nm. In order to reduce random error and noise, each spectrum was an average of five scans over 250–200 nm.

Background spectra were acquired using the same buffer as used for the protein samples. The spectra were corrected for the baseline and normalized to the amino acid concentration in order to obtain the mean residue molar ellipticity (deg cm²/dmol). Denaturation studies were carried out using urea of 2–8 M concentration.

Secondary structure estimation. The experimental CD spectra were processed in order to estimate the contribution of different secondary structural elements [17]. The percentages of α -helix, β -sheet, and coil were calculated using the standard secondary structure analysis program provided with Jasco-810 spectropolarimeter.

Fluorescence measurements. The steady-state fluorescence measurements were performed with a SPEX Fluorolog-3 spectrofluorometer at 22 °C. The fluorescence was measured with a 10 mm quartz cuvette. The samples were excited at 280 nm with the excitation and emission bandwidths at 5 and 2 nm, respectively. The spectra were blank subtracted. Each spectrum was corrected for monochromator efficiency. To eliminate the effect of lamp intensity variation during the time of measurement all spectra were recorded with S/R setting. Protein solutions (~1 µM) contained 20 mM phosphate and 300 mM NaCl at pH 7.0. The acrylamide stock solution (1 M) was freshly made in phosphate buffer (20 mM phosphate and 300 mM NaCl, pH 7.0) containing 1 µM protein. The quenching studies of the denatured protein were performed in the presence of 6 M urea. The acrylamide stock solution (1 M) was made in the same buffer containing 6 M urea. The fluorescence intensity was measured at 340 nm in the case of native protein and at 355 nm for the denatured protein samples. The analysis of acrylamide quenching data was made using non-linear least-squares fitting to $F_0/F = (1 + K_{SV}[Q]) \exp(V/[Q])$, where F_0 and F are fluorescence intensities in the absence and presence of quencher Q , K_{SV} is the Stern–Volmer collisional quenching constant, and V is the static quenching constant.

The denaturation of the protein was carried out by use of fluorescence titration method. Stock solutions of 8 M urea or 6 M guanidine hydrochloride were made in the same buffer containing 1 µM protein. A 2.5 ml volume of the protein solution was titrated manually with the respective denaturant in the quartz cuvette. The solutions were excited at 280 nm and the fluorescence intensity was measured at 340 nm.

Molecular modeling. A restraint based modeling program MODELLER 6v0 [18] was used for generating the model of RecX. This program uses an automated approach to comparative modeling by the satisfaction of spatial restraints [19,20].

The secondary structure of the target sequence was identified using different algorithms like PSIPRED [21] and PHD [22]. Since the target sequence of RecX of *E. coli* was not significantly similar to any protein of known 3D structure in PDB database, fold recognition techniques (3D-PSSM [23], GenTHREADER [24], BIOINBGU [25], FUGUE [26], and FFAS [27]) were used to identify other candidates having similar folds. The most cited folds were identified at low E -values by the fold recognition method and selected. Then the target sequence was aligned with sequences of related known three-dimensional structures (templates) having similar folds.

The coordinates of the structure of protein with PDB code 1ku2a were assigned to the target sequence according to an alignment resulting from the threading and manually refined on the basis of the consensus secondary structure prediction and structural details of 1ku2a. MODELLER built a three-dimensional model of the target sequence containing all main chain and side chain non-hydrogen atoms. The whole model, including backbone, side chains, and loops, was built in one optimization.

The best model was evaluated externally and internally on the basis of stereochemistry and energy of minimization, which reduces the steric hindrance. The optimization was carried out by the use of the variable target function method [28] employing methods of conjugate gradients (CG) and steepest descent (SD). Four hundred different models were calculated by varying the initial structure. The final model was selected based on stereochemical quality and energy value.

Analysis of the model. The overall stereochemical quality of the final model for RecX was assessed by PROCHECK [29] and ERRAT [30].

Docking of RecX to RecA. The hexameric RecA was generated using crystallographic 6_1 symmetry applied on the coordinates of the RecA monomer deposited in the Protein Data Bank, 2REB. The hexameric assembly and RecX were docked using GRAMM v1.03 [31] to find out the binding mode of RecX to RecA.

Results and discussion

Expression and purification of RecX

Overexpression of the soluble form of the protein was optimized at 20 °C and 0.25 mM IPTG concentration. Gel filtration chromatography showed a single peak corresponding to the monomeric form (~22 kDa) (Fig. 1). The molecular mass of RecX was also measured with Voyager-DE PRO MALDI-TOF mass spectrometer and data were analyzed giving a value of 21780.99 Da which is close to the expected value of monomeric form.

Modeling of RecX

BLAST sequence alignment of the protein sequence against the PDB database showed no significant confidence level or similarity of RecX with any other protein. Hence fold prediction techniques were used to overcome the limited availability of structural information by predicting the 3D fold of the protein. All the fold prediction methods used, ranked σ factor protein, 1ku2a [32], within the top ten positions. Again, secondary structure prediction by PSIPRED and PHD suggested the topology of the target protein to be mainly α helical. The σ factor protein is mostly helical and it has DNA binding activity. Hence 1ku2a was selected as the template on the basis of structure. Spatial restraints of α -helix from 10–40, 50–65, 71–85, 90–100, 104–114, 116–130, 138–150, and 155–164 residues were extracted from the alignment of the target sequence with the template structure. Twenty models of RecX were generated by MODELLER.

The model of lowest energy value, containing only 89.5% core region, was taken for further energy minimization and simulation. The quality of the model was improved by running different cycles (100, 200, 300, and 400) of SD and CG simultaneously. Conditions required were optimized and the best model was obtained after 300 cycles of SD. The core region of the final model increased to 98% with no disallowed regions.

Analysis of the Ramachandran plot of the energy minimized model (Fig. 2) showed that 90.1% of the residues were in the most favorable regions and 8.6% in the additional allowed regions.

Structural characterization and validation of the model

Multiple sequence alignment (Fig. 3) of seven bacterial RecX proteins showed no significant similarity between the sequences. Thus the interaction between RecA and

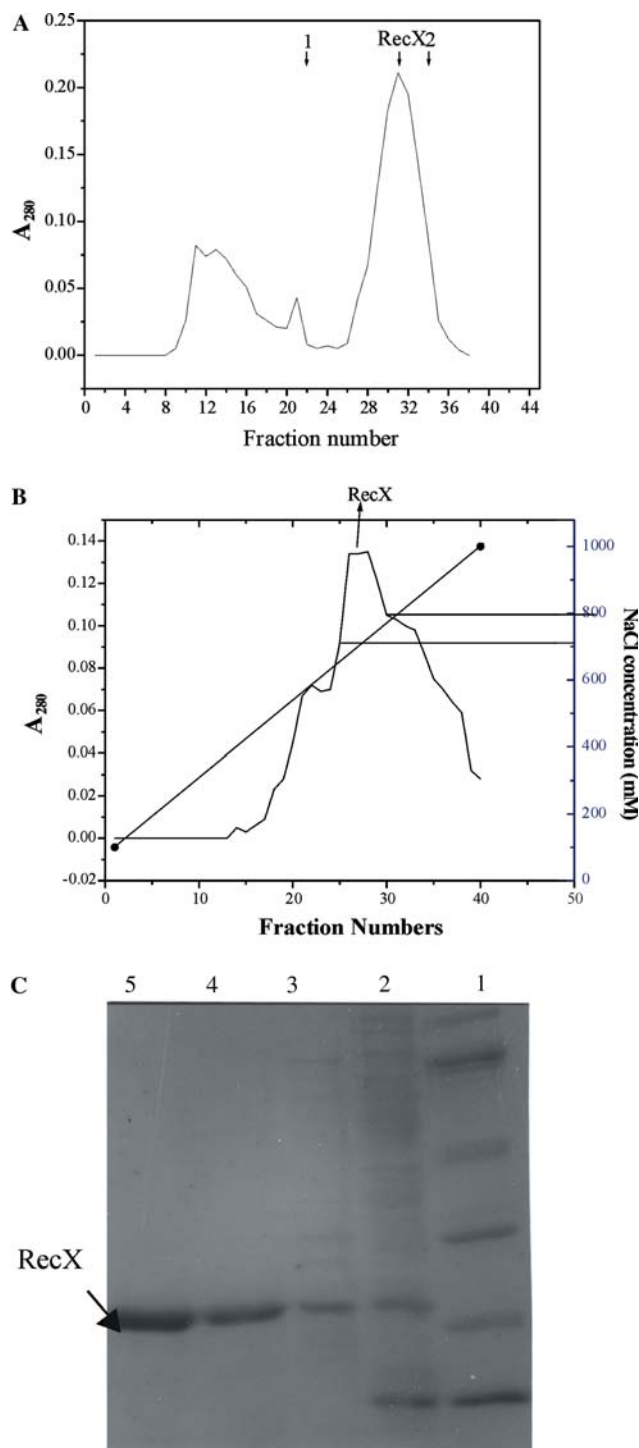


Fig. 1. (A) Gel filtration chromatogram using Sephadex G-75. The elution profiles of BSA (1) and lysozyme (2) are shown by arrows. (B) Mono-S chromatogram. (C) Coomassie blue stained 15% SDS-PAGE at different purification steps correspond to: molecular weight markers (lane 1, kDa) 14.5, 21.5, 26.6, 39.2, and 66.2; whole cell (lane 2); purified fraction from Ni-NTA (lane 3); pooled fraction from gel filtration (lane 4); Mono-S (lane 5).

RecX is highly variable and species-specific. Modeling (Figs. 4A and B) showed RecX to be a nine helical bundle protein consisting of two domains. The smaller

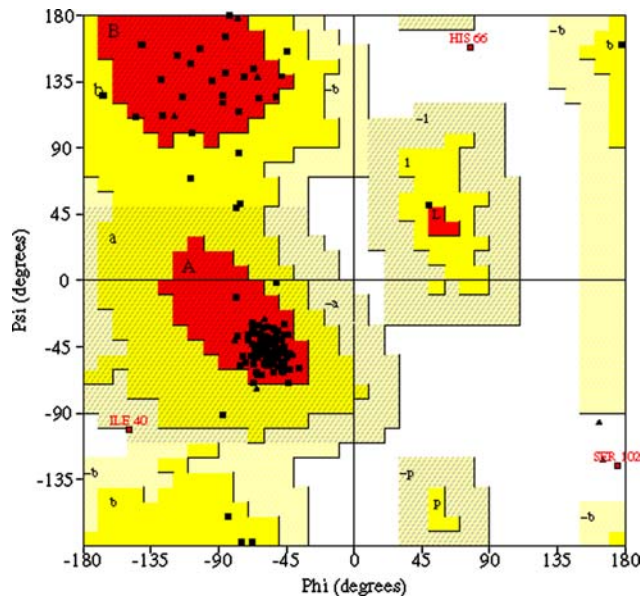


Fig. 2. Ramachandran plot of modeled RecX.

C-terminal domain has two amphipathic helices with a helix turn helix motif and is stabilized by hydrophobic interactions between Phe 165, Trp 162, Phe 138, and Lys 141. The folding is stabilized by hydrophilic interactions between the two domains. There is no significant cross-

over angle among the helices which indicates the absence of superhelical coils in the molecule. The electrostatic potential surface of RecX, calculated using GRASP [33] (Fig. 4C), indicated a mostly neutral surface. Docking of RecX into RecA hexamer shows that RecX binds to a tandem array of three consecutive RecA molecules at its ATP binding site which is close to its DNA binding site.

The extinction coefficient of RecX has been determined as $44 \times 10^3 \text{ M}^{-1} \text{ cm}^{-1}$ which is higher than that of myoglobin, a protein with the same molecular weight. This indicates the elongated form of an RecX structure. A broad negative band with a minimum at 220 nm in the results obtained from far UV CD scan, and the peak at 1649.1 cm^{-1} (results not shown) in the amide I transition from FTIR spectroscopy supported the high propensity of helical structures in RecX. Secondary structure analysis of CD spectra showed the α -helix, β -sheet, and random coil content of RecX to be about 25%, 0%, and 48.06%, respectively, with 32.7% turns. The urea denaturation profile (Fig. 5A) of RecX measured by acquiring CD spectra as a function of the urea concentration (from 2 to 8 M) showed the protein to be stable up to 2 M urea. In order to monitor the melting of the protein, the residue molar ellipticity at 220 nm for each concentration of urea was recorded (Fig. 5B).

The normalized fluorescence spectra (not shown here) of the protein for excitation at 275 and 295 nm were

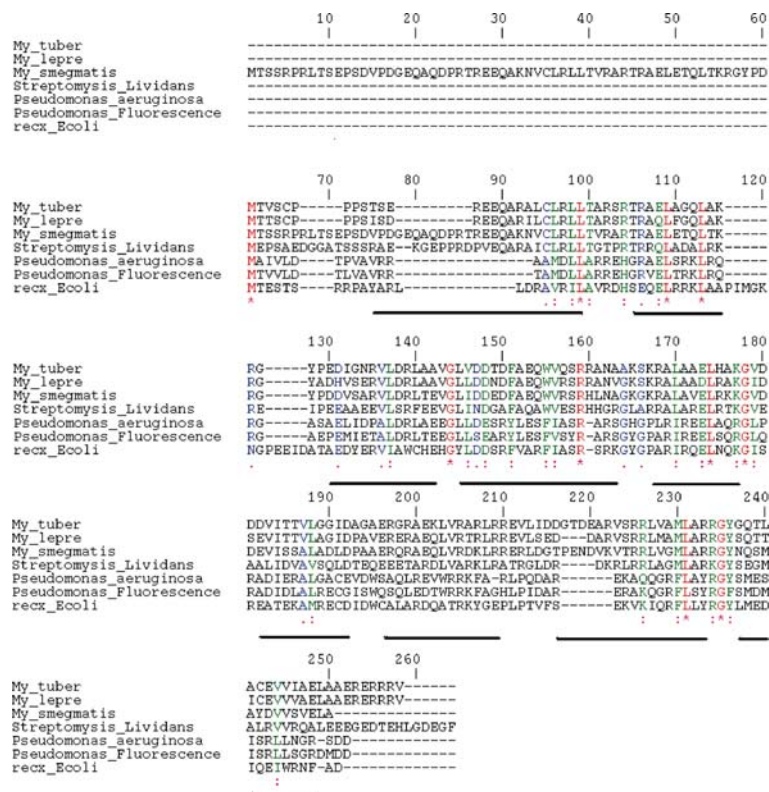


Fig. 3. Multiple sequence alignment of RecX. Residues that are invariant in all sequences are colored red. Conserved residues (which are mostly hydrophobic) are in green and in blue. Helices are indicated by black lines. (For interpretation of the references to color in this figure legend, the reader is referred to the web version of this paper.)

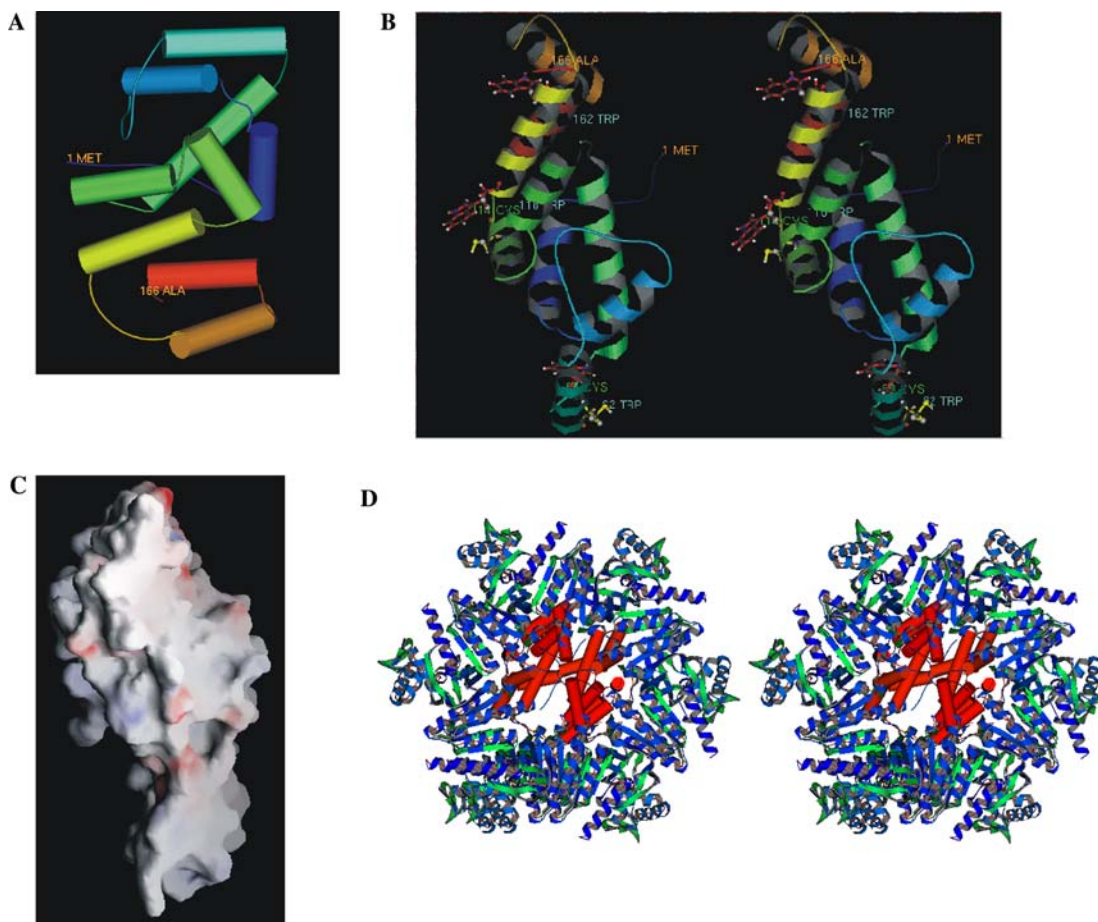


Fig. 4. (A) Architecture of RecX. (B) Stereoview showing solvent accessibility of the tryptophan residues. (C) Electrostatic surface charge potential of molecular surface of RecX generated with GRASP. (D) Interaction of RecX with RecA. RecX molecules are shown in red with the helices depicted in cylindrical form. The figure was produced using MOLSCRIPT [36]. (For interpretation of the references to color in this figure legend, the reader is referred to the web version of this paper.)

identical. This implies that the contribution of the tyrosine fluorescence to the protein fluorescence is negligible. Therefore, for all fluorescence measurements, the solutions were excited at 280 nm. The fluorescence spectra of the native and unfolded protein are depicted in the inset of Fig. 6A. The spectrum corresponding to the native protein ($\lambda_{\text{max}} = 339$ nm) is blue-shifted relative to that of the unfolded protein ($\lambda_{\text{max}} = 355$ nm) and suggests that the tryptophan molecules are located within a less polar environment in the native protein than in the unfolded state. This is also manifested by the fluorescence intensity of the unfolded protein, which is less than that in the native protein. However, the broad spectrum indicates that the spectrum of the native protein is composite of all the spectra due to different tryptophan molecules located in different environments. To further investigate the microenvironments of the tryptophan molecules both the native and unfolded proteins were subjected to acrylamide quenching. Acrylamide is a water-soluble quencher and therefore, only fluorescence of those tryptophan molecules, which are

exposed to the bulk solvent, is expected to be quenched. Indeed, the fluorescence spectra of both the native and denatured proteins almost disappeared in the presence of high concentration of acrylamide. The modified Stern–Volmer plots for the fluorescence quenching are shown in Fig. 6A. The quenching data are listed in Table 1. As depicted by the curvilinear response both the native and denatured proteins exhibited dynamic as well as static components in their quenching by acrylamide. The upward curvature of the plots suggested that all the tryptophanyl residues are equally accessible to the quencher molecules. This is also indicated by the large values of static quenching constant. The static quenching constants, within the limits of experimental error, are equal. The value of V also provides insight into the relative exposure of the tryptophanyl residue. A value of 5.7 M^{-1} indicates full solvent exposure of the tryptophanyl residues. The dynamic quenching constant for the denatured protein is almost three times that of native protein. The kinetic data of the quenching processes may also be valuable in determining the solvent

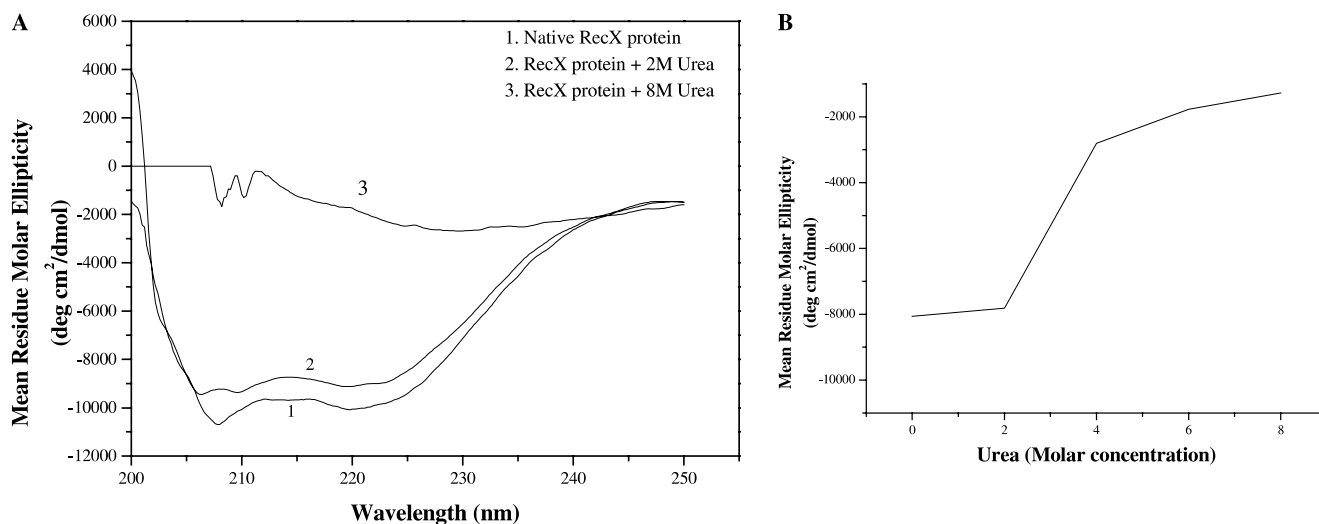


Fig. 5. Circular dichroism spectra (A) increasing concentration of urea (from 0 to 8 M). (B) Melting curves of RecX.

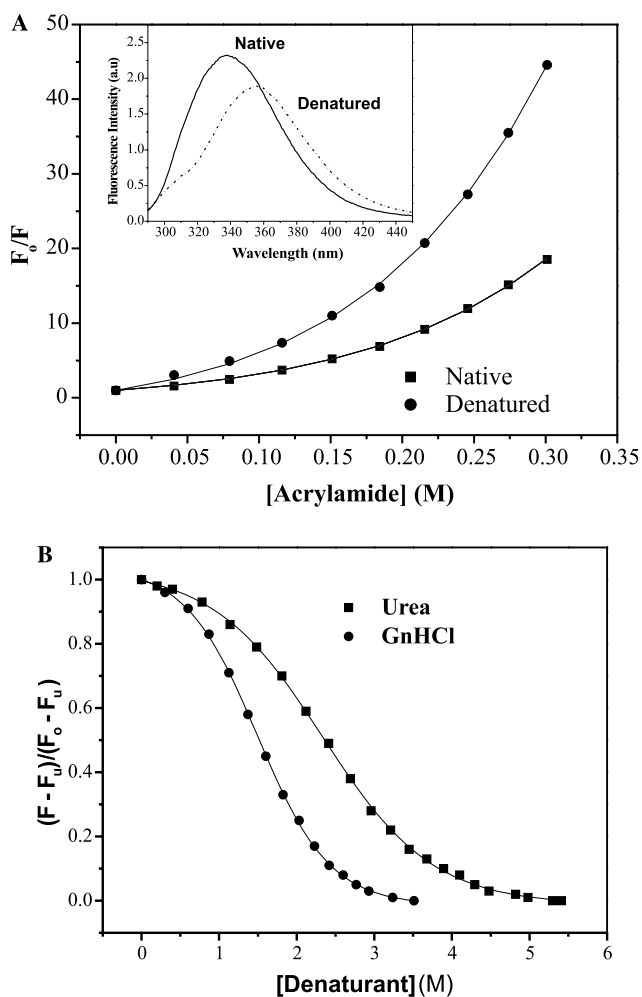


Fig. 6. (A) Modified Stern–Volmer plot for fluorescence quenching of native and denatured proteins by acrylamide. (Inset) Fluorescence spectra of native and denatured proteins. (B) Denaturation of the native protein by urea and GdnHCl.

Table 1

Fluorescence quenching data of the native and denatured proteins

Protein	K_{SV}	V (M^{-1})	$k_q \times 10^{-9}$ (s^{-1})
Native	7.7	5.7	5.5
Denatured	24.1	5.6	17.2

exposure of the tryptophanyl residues. If the average lifetime of the tryptophan fluorescence is assumed to be 1.4 ns [34,35], then the rate constant of quenching becomes equal to ~ 5.5 and $17.2 \times 10^9 s^{-1}$, respectively, for the native and denatured proteins. These values are very close to the diffusion limit and suggest that the tryptophanyl residues in both the proteins are fully exposed to water. This supports the modeled structure of the native protein. It can be seen in Fig. 4 that in the native protein, there are several channels through which water molecules can penetrate and can interact with the tryptophan residues.

That the native protein has several solvent channels is also indicated by the results of protein denaturation studies. Denaturation of the protein has been studied using urea and guanidine hydrochloride as denaturant. The titration curves are shown in Fig. 6B. The titration curves resemble those corresponding to a two-state equilibrium. Therefore it suggests that the transition occurs between the native and unfolded state of the protein only. The inflection points of the curves *A* and *B* correspond to 1.6 M GdnHCl and 2.4 M urea, respectively, i.e., for 50% denaturation of the protein only 1.6 M GdnHCl or 2.4 M urea is required. These values are relatively low compared to the corresponding values observed for other proteins of similar size. The low values of denaturant required to unfold the native protein clearly suggest that the protein is relatively unstable justifying the modeled structure in Fig. 4.

Interaction of RecX with RecA

The biologically active form of RecA is a helical hexamer ~120 Å wide with a central diameter of 25 Å consisting of three domains, a major central domain, smaller amino terminal, and carboxy domains. The central domain of RecA is believed to be involved in ATP, ssDNA, and duplex DNA binding. The enzyme works through the formation of a RecA–ssDNA–ATP nucleoprotein filament. The DNA binding regions of RecA are highly conserved. Overexpression of RecX in *E. coli* has been found to inhibit coprotease and recombinase activities of RecA thus affecting the SOS response and also DNA strand exchange. Here we have tried to establish the mode of regulation of RecA by RecX.

RecX simultaneously interacts with the ATP binding site of RecA as well the DNA binding sites, i.e., L1 (157–164) and L2 (195–209) regions. These regions are closer to the crystallographic 6_1 screw axis of RecA and lie towards the innermost face of the hexamer with L2 lying directly above the ATP binding site. The docked structure (Fig. 4D) indicates that RecX, having a width of 24.98 Å, enters the filamentous RecA molecule horizontally along the spiral direction of the RecA molecule. Part of the RecX molecule sits on the RecA filament at its ATP binding site thus inhibiting entry of the substrate reducing its ATPase activity and the remaining part of RecX stacks along the helix axis, competing with and preventing the vertical entry of the DNA molecule. This in turn inhibits the DNA strand exchange promoting function of RecA. Inhibition of ATPase activity through binding of RecX with RecA disturbs the equilibrium between SSB (single stranded binding protein) and RecA binding to ssDNA. This inhibits DNA strand exchange, RecA recombinase activity and also inhibits coprotease activity, i.e., self-cleavage of LexA and UmuD in turn inhibiting SOS response.

Acknowledgments

This work was supported by grants from the Department of Biotechnology, Government of India and CSIR, New Delhi. S.M. and P.A.M. were supported by Senior Research Fellowships from CSIR, New Delhi, India.

References

- [1] S.F. Altschul, W. Gish, W. Miller, E.W. Myers, D.J. Lipman, Basic local alignment search tool, *J. Mol. Biol.* 215 (1990) 403–410.
- [2] S. Karlin, G.M. Weinstock, V. Brendel, Bacterial classifications derived from RecA protein sequence comparisons, *J. Bacteriol.* 177 (1995) 6881–6893.
- [3] S. Karlin, L. Brocchieri, Evolutionary conservation of *recA* genes in relation to protein structure and function, *J. Bacteriol.* 178 (1996) 1881–1894.
- [4] B. Nubbaumer, W. Wohlleben, Identification, isolation and sequencing of the *recA* gene of *Streptomyces lividans* TK24, *FEMS Microbiol. Lett.* 118 (1994) 57–64.
- [5] R.M. Story, I.T. Weber, T.A. Steitz, The structure of the *E. coli* recA protein monomer and polymer, *Nature* 355 (1992) 318–324.
- [6] N. Guiliani, A. Bengrine, F. Borne, M. Chippaus, V. Bonnefoy, Alanyl-tRNA synthetase gene of the extreme acidophilic chemolithoautotrophic *Thiobacillus ferrooxidans* is highly homologous to *alaS* genes from all living kingdoms but cannot be transcribed from its promoter in *Escherichia coli*, *Microbiology* 143 (1997) 2179–2187.
- [7] Y. Sano, Role of the *recA*-related gene adjacent to the *recA* gene in *Pseudomonas aeruginosa*, *J. Bacteriol.* 175 (1993) 2451–2454.
- [8] R. De Mot, G. Schoofs, J. Vanderleyden, A putative regulatory gene downstream of *recA* is conserved in Gram-negative and Gram-positive bacteria, *Nucleic Acids Res.* 22 (1994) 1313–1314.
- [9] K.G. Papavinasasundaram, F. Movahedzadeh, J.T. Keer, N.G. Stoker, M.J. Colston, E.O. Davis, Mycobacterial *recA* is cotranscribed with a potential regulatory gene called *recX*, *Mol. Microbiol.* 24 (1997) 141–153.
- [10] E. Zaitsev, A. Alexseyev, V. Lanzov, L. Satin, A.J. Clark, Nucleotide sequence between *recA* and *alaSp* in *E. coli* K12 and the sequence change in four *recA* mutations, *Mutat. Res.* 323 (1994) 173–177.
- [11] K.G. Papavinasasundaram, M.J. Colston, E.O. Davis, Construction and complementation of a *recA* deletion mutant of *Mycobacterium smegmatis* reveals that the intein in *Mycobacterium tuberculosis recA* does not affect RecA function, *Mol. Microbiol.* 3 (1998) 525–534.
- [12] R. Venkatesh, N. Ganesh, N. Guhan, M.S. Reddy, T. Chandrasekhar, K. Muniyappa, RecX protein abrogates ATP hydrolysis and strand exchange promoted by RecA: insights into negative regulation of homologous recombination, *Proc. Natl. Acad. Sci. USA* 99 (2002) 12091–12096.
- [13] E.A. Stohl, J. Brockman, K.L. Burkle, K. Morimatsu, S.C. Kowalczykowski, S. Seifert, *Escherichia coli* RecX inhibits RecA recombinase and coprotease activities in vitro and in vivo, *J. Biol. Chem.* 278 (2003) 2278–2285.
- [14] E.A. Stohl, L. Blount, H.S. Seifert, Differential cross-complementation patterns of *Escherichia coli* and *Neisseria gonorrhoeae* RecA proteins, *Microbiology* 148 (2002) 1821–1831.
- [15] M.M. Bradford, A rapid and sensitive for the quantitation of microgram quantities of protein utilizing the principle of protein-dye binding, *Anal. Biochem.* 72 (1976) 248–254.
- [16] C.M. Stoscheck, Quantitation of the protein, *Methods Enzymol.* 182 (1990) 50–69.
- [17] N.J. Greenfield, Methods to estimate the conformation of proteins and polypeptides from circular dichroism data, *Anal. Biochem.* 235 (1996) 1–10.
- [18] A. Sali, T.L. Blundell, Comparative protein modelling by satisfaction of spatial restraints, *J. Mol. Biol.* 234 (1993) 779–815.
- [19] A. Sali, J.P. Overington, Derivation of rules for comparative protein modeling from a database of protein structure alignments, *Protein Sci.* 3 (1994) 1582–1596.
- [20] A. Sali, L. Potterton, F. Yuan, H.V. Vlijmen, M. Karplus, Evaluation of comparative protein modeling by MODELLER, *Proteins* 23 (1995) 318–326.
- [21] L.J. McGuffin, K. Bryson, D.T. Jones, The PSIPRED protein structure prediction server, *Bioinformatics* 16 (2000) 404–405.
- [22] B. Rost, C. Sander, R. Schneider, PHD—an automatic mail server for protein secondary structure prediction, *CABIOS* 10 (1994) 53–60.
- [23] L.A. Kelley, R.M. MacCallum, M.J.E. Sternberg, Enhanced genome annotation using structural profiles in the program 3D-PSSM, *J. Mol. Biol.* 299 (2000) 501–522.
- [24] D.T. Jones, GenTHREADER: an efficient and reliable protein fold recognition method for genomic sequences, *J. Mol. Biol.* 287 (1999) 797–815.

- [25] J. Osuna, X. Soberon, E. Morett, A proposed architecture for the Central domain of the bacterial enhancer-binding proteins based on secondary structure prediction and fold recognition, *Protein Sci.* 6 (1997) 543–555.
- [26] J. Shi, T.L. Blundell, K. Mizuguchi, FUGUE: sequence-structure homology recognition using environment-specific substitution tables and structure-dependent gap penalties, *J. Mol. Biol.* 310 (2001) 243–257.
- [27] L. Rychlewski, L. Jaroszewski, W. Li, A. Godzik, Comparison of sequence profiles: strategies for structural predictions using sequence information, *Protein Sci.* 9 (2000) 232–241.
- [28] W. Braun, N. Go, Calculation of protein conformations by proton–proton distance constraints. A new efficient algorithm, *J. Mol. Biol.* 186 (1985) 611–626.
- [29] R.A. Laskowski, M.W. MacArthur, D.S. Moss, J.M. Thornton, PROCHECK: a program to check the stereochemical quality of protein structures, *J. Appl. Crystallogr.* 26 (1993) 283–291.
- [30] C. Colovos, T.O. Yeates, Verification of protein structures: patterns of nonbonded atomic interactions, *Protein Sci.* 2 (1993) 1511–1519.
- [31] I.A. Vakser, C. Aflalo, Hydrophobic docking: a proposed enhancement to molecular recognition techniques, *Proteins* 20 (1994) 320–329.
- [32] E.A. Campbell, O. Muzzin, M. Chlenov, J.L. Sun, C.A. Olson, O. Weinman, M.L. Trester-Zedlitz, S.A. Darst, Structure of the bacterial RNA polymerase promoter specificity sigma subunit, *Mol. Cell* 9 (2002) 527–539.
- [33] A. Nicholls, K.A. Sharp, B. Honig, Protein folding and association: insights from the interfacial and thermodynamic properties of hydrocarbons, *Proteins: Struct. Funct. Genet.* 11 (1991) 281–296.
- [34] F. Strasser, J. Dey, M.R. Eftink, B.V. Plapp, Activation of horse liver alcohol dehydrogenase upon substitution of Tryptophan 314 at the dimer interface, *Arch. Biochem. Biophys.* 358 (1998) 369–376.
- [35] H.K. Brandes, F.W. Larimer, Tse-Yuan S. Lu, J. Dey, F.C. Hartman, Roles of microenvironments of tryptophanyl residues of spinach phosphoribulokinase, *Arch. Biochem. Biophys.* 352 (1998) 130–136.
- [36] B.L. Kraulis, MOLSCRIPT: a program to produce both detailed and schematic plots of protein structures, *J. Appl. Crystallogr.* 24 (1991) 946–950.